DESY 94-128
SCIPP 94/20
August 1994

Azimuthal Angle Decorrelation in Large-rapidity Dijet Production at the Tevatron[a]

Vittorio Del Duca
Deutsches Elektronen-Synchrotron
DESY, D-22607 Hamburg , GERMANY

and

Carl R. Schmidt [b]
Santa Cruz Institute for Particle Physics
University of California, Santa Cruz, CA 95064, USA

Abstract

In this talk we examine the azimuthal angle decorrelation in dijet production at large rapidity intervals at the Tevatron as a possible signature of the BFKL evolution.

---

[a]Invited talk presented by V.D.D. at the "QCD 94" workshop, Montpellier, France, July 7-13, 1994

[b]Supported in part by the U.S. Department of Energy.

1 Introduction

The state-of-the-art in jet physics at hadron colliders is described by next-to-leading-order (NLO) QCD parton-level calculations[1], [2], [3]. They appear to be in very good agreement with the one- and two-jet inclusive distributions obtained from the data of the CDF experiment at the Fermilab Tevatron Collider[4], [5]. However, since data are being collected at the CDF and D0 detectors at larger and larger rapidities, it may be possible to probe kinematic configurations where this fixed-order analysis is inadequate. This could occur when the cross section contains logarithms of large ratios of kinematic invariants. Typical invariants are the hadron-hadron center-of-mass energy $\sqrt{s}$, the parton-parton center-of-mass energy $\sqrt{\hat{s}} = \sqrt{x_A x_B s}$, where x_A and x_B are the momentum fractions of the partons originating the hard scattering, and the momentum transfer Q, which is of the order of the transverse momentum of the jets produced in the hard scattering. If x_A and x_B are large, then the large logarithms, $\ln(\hat{s}/Q^2)$, factorize into the partonic subprocess cross section. These logarithms, which are of the size of the rapidity interval in the scattering process, can be resummed by using the techniques of Balitsky, Fadin, Kuraev, and Lipatov (BFKL)[6].

In analyzing dijet production experimentally so that it most closely resembles the configuration assumed in the BFKL theory, the jets are ordered first by their rapidity rather than by their energy[7]. Thus, we look at all the jets in the event that are above a transverse momentum cutoff $p_{\perp min}$, using some jet-definition algorithm, and rank them by their rapidity. We then tag the two jets with the largest and smallest rapidity and observe the distributions as a function of these two *tagging jets*. The cross section is inclusive so that the distributions are affected by the hadronic activity in the rapidity interval y between the tagging jets, whether or not these hadrons pass the jet-selection criteria. We will refer to these hadrons in the rapidity interval as *minijets*. For dijet events at large rapidity intervals the BFKL theory systematically resums the leading powers in the rapidity interval y, including both real and virtual gluon corrections.

In ref. [8] we showed that the exponential enhancement with y in dijet production at fixed x_A and x_B , originally suggested as a signature of the BFKL minijets by Mueller and Navelet[7], is highly suppressed by the parton distribution functions at Tevatron energies. However, we found that other observables such as the transverse momentum $p_\perp$ distribution and the jet-jet correlations in $p_\perp$ and azimuthal angle ϕ are significantly affected by the minijet resummation. For example, we saw that these correlations are not a leading feature of the expansion in the rapidity interval. Accordingly, they fade away as the rapidity interval increases.

However, in comparing the BFKL resummation with the exact $\mathcal{O}(\alpha_s^3)$ calculation[9], we noticed that the large-rapidity approximation to the kinematics causes a serious error in the BFKL predictions when the tagging jets are not back-to-back in $p_\perp$ and ϕ. In order to account for this error we introduced an effective rapidity $\hat{y}$ which restricts the phase space of the minijets in such a way that the truncation of the BFKL resummation to $\mathcal{O}(\alpha_s^3)$ agrees with the exact $2 \to 3$ $\mathcal{O}(\alpha_s^3)$ calculation. For large y, the difference $y - \hat{y}$ is nonleading. Since the rapidity variable which is resummed by BFKL is only defined up to transformations $y \to y + X$ where X is subleading at large rapidities, we used $\hat{y}$ instead of y in the BFKL resummation in order to obtain quantitatively more reliable predictions of the transverse momentum distributions. We use here the effective rapidity $\hat{y}$ in the BFKL resummation to analyze the moments[10] of the decorrelation in azimuthal angle.

2 The minijet resummation and the effective rapidity interval

We are interested in the semi-inclusive production of two jets in hadron-hadron collisions $p_A \bar{p}_B \to j_1 j_2 + X$. We describe the two partonic tagging jets by their transverse momenta and rapidities $(\vec{p}_{1\perp}, y_1)$ and $(\vec{p}_{2\perp}, y_2)$, where we always take $y_1 > y_2$. We reexpress the jet rapidities in terms of the rapidity interval $y = y_1 - y_2$ and the rapidity boost $\bar{y} = (y_1 + y_2)/2$. This is convenient since we are mainly interested in the behavior of the parton subprocess, which does not depend on $\bar{y}$. For large values of y the cross section for this process can be written

$$\frac{d\sigma_0}{dy\, d\bar{y}\, dp_{1\perp}^2 dp_{2\perp}^2 d\phi} = x_A^0 x_B^0\, f_{\rm eff}(x_A^0, \mu^2) f_{\rm eff}(x_B^0, \mu^2)\, \frac{d\hat{\sigma}_{gg}}{dp_{1\perp}^2 dp_{2\perp}^2 d\phi}\,, \qquad (1)$$

where the parton momentum fractions are dominated by the contribution from the two tagging jets

$$\begin{aligned} x_A^0 &= \frac{p_{1\perp} e^{y_1}}{\sqrt{s}} \\ x_B^0 &= \frac{p_{2\perp} e^{-y_2}}{\sqrt{s}}, \end{aligned} \qquad (2)$$

and μ is the factorization/renormalization scale. In this limit the amplitude is dominated by gg, qg, and qq scattering diagrams with gluon-exchange in the t-

channel. The relative magnitude of the different subprocesses is fixed by the color strength of the respective jet-production vertices, so it suffices to consider only gg scattering and to include the other subprocesses by means of the effective parton distribution function $f_{\rm eff}(x,\mu^2)$ [11],[7].

The higher-order corrections to the gg subprocess cross section in (1) can be expressed via the solution of the BFKL equation[6], which is an all-order resummation in α_s of the leading powers of the rapidity interval

$$\frac{d\hat\sigma_{gg}}{dp_{1\perp}^2 dp_{2\perp}^2 d\phi} = \frac{C_A^2\alpha_s^2}{4\pi p_{1\perp}^3\, p_{2\perp}^3} \sum_n e^{in(\phi-\pi)} M_n(y, p_{1\perp}, p_{2\perp}) \tag{3}$$

with

$$M_n(y, p_{1\perp}, p_{2\perp}) = \int_0^\infty d\nu e^{\omega(n,\nu)\,y} \cos\left(\nu\, \ln\frac{p_{1\perp}^2}{p_{2\perp}^2}\right) \tag{4}$$

and

$$\omega(n,\nu) = \frac{2C_A\alpha_s}{\pi}[\psi(1) - {\rm Re}\,\psi(\frac{|n|+1}{2} + i\nu)], \tag{5}$$

and ψ the logarithmic derivative of the Gamma function. Eq. (3) can be expanded order by order in α_s. At $\mathcal{O}(\alpha_s)$ and for $p_{1\perp} \neq p_{2\perp}$ we obtain

$$\frac{d\hat\sigma_{gg}^{(1)}}{dp_{1\perp}^2 dp_{2\perp}^2 d\phi} = \frac{C_A^2\alpha_s^2}{4\pi p_{1\perp}^2\, p_{2\perp}^2}\, \frac{C_A\alpha_s y}{p_{1\perp}^2 + p_{2\perp}^2 + 2p_{1\perp}p_{2\perp}\cos\phi}. \tag{6}$$

This can be compared with a fixed-order calculation of dijet production at the same order of α_s, computed through the 2$\to$3 parton amplitudes,

$$\frac{d\sigma}{dy\, d\bar y\, dp_{1\perp}^2\, dp_{2\perp}^2\, d\phi} = \int_{y_2}^{y_1} dy_3 \int \sum_{ij} x_A x_B f_{i/A}(x_A,\mu^2) f_{j/B}(x_B,\mu^2)\, \frac{d\hat\sigma_{ij}}{dp_{1\perp}^2 dp_{2\perp}^2 dy_3 d\phi}\ , \tag{7}$$

where y_3 is the rapidity of the third final-state parton, integrated over the interval spanned by the tagging jets. $f_{i(j)} = Q, \bar Q, G$ labels the distribution function of the parton species and flavor $i(j) = q, \bar{q}, g$ inside hadron $A(B)$. We include all parton subprocesses[12], and use the exact values of the parton momentum fractions

$$
\begin{aligned}
x_A &= \frac{p_{1\perp} e^{y_1} + p_{2\perp} e^{y_2} + p_{3\perp} e^{y_3}}{\sqrt{s}} \\
x_B &= \frac{p_{1\perp} e^{-y_1} + p_{2\perp} e^{-y_2} + p_{3\perp} e^{-y_3}}{\sqrt{s}} .
\end{aligned} \tag{8}
$$

In order to avoid the collinear singularity between final-state partons, which is however subleading at large rapidities[9], configurations in (7) where the distance R between two of the partons on the Lego plot in azimuthal angle and rapidity is smaller than the jet cone size R_{cut} are discarded. In the large-y limit (7) reduces to (1), with the parton cross section given by (6).

However, we have seen in ref.[9] that the large-y approximation seriously over-estimates the cross section when the two tagging jets are not back-to-back in $p_\perp$ and ϕ, even for rapidity intervals as large as $y = 6$. This occurs because the large-y cross section (6) assumes that the third (minijet) parton can be produced anywhere within the rapidity interval $[y_2, y_1]$ with equal probability, whereas in the full $2 \to 3$ cross section the probability is highly suppressed by the structure functions when the third jet strays too far from the center of this interval. In ref.[9] we introduced an "effective" rapidity interval $\hat{y}$ to take into account the fact that the range in rapidity spanned by the minijets is typically less than the kinematic rapidity interval y. We define $\hat{y}(n, p_{1\perp}, p_{2\perp}, \bar{y}, y)$ by

$$
\hat{y} \equiv y \frac{\int d\phi \cos(n\phi) \ (d\sigma / dy d\bar{y} dp_{1\perp} dp_{2\perp} d\phi)}{\int d\phi \cos(n\phi) \ (d\sigma_0 / dy d\bar{y} dp_{1\perp} dp_{2\perp} d\phi)}, \tag{9}
$$

where n is the Fourier series index of eq. (3). The cross section in the numerator is that of eq. (7) and is computed using the exact kinematics (8), while the cross section in the denominator is that of eq. (1) and is computed using the large-y kinematics (2). The denominator can easily be computed analytically using the large-y solution (6). Note that $\hat{y}$ is defined so that if we replace $y \to \hat{y}$ in the BFKL solution (3) and truncate to $\mathcal{O}(\alpha_s^3)$ we recover the exact $2 \to 3$ cross section.

3 The azimuthal angle decorrelation

Our aim is now to reconsider the azimuthal angle decorrelation[8],[10] by using the effective rapidity $\hat{y}$ instead of the kinematic one y in the BFKL resummation. Using $\hat{y}$, we expect that the distribution will be more populated around the peak $\phi = \pi$ where the tagging jets are back-to-back, and less populated on its tails where the tagging jets are decorrelated, as compared to the ϕ decorrelation plot we considered in ref.[8]. This is because the larger the decorrelation, the larger the overestimating error in approximating the parton momentum fractions with eq. (2). However, in practice the computation of the Fourier coefficients (4) using eq. (9) for $\hat{y}$ becomes quickly very time-consuming as n grows. To test the BFKL picture, it is then more convenient to compute the moments of the azimuthal angle[10], defined by

$$< \cos n(\phi-\pi) > = \frac{\int_0^{2\pi} d\phi \cos n(\phi-\pi) \, (d\sigma_0/dy d\phi)}{\int_0^{2\pi} d\phi (d\sigma_0/dy d\phi)}. \qquad (10)$$

For a δ-function distribution at $\phi = \pi$, as occurs at the Born level, all of the moments will equal one, while for a flat distribution all of the moments will equal zero for $n \geq 1$. Thus, the decay of the moments from unity is a good measure of the decorrelation in ϕ.

In Fig. 1 we plot in the solid curves the first two moments of the azimuthal angle as a function of y, calculated using the effective rapidity $\hat{y}$ in the BFKL solution. We use the LO CTEQ2 parton distribution functions[13] with the ren./fact. scales set to $\mu^2 = p_{1\perp} p_{2\perp}$. To facilitate the comparison with the experimental data we choose the kinematic parameters of the data analysis of the 1993 run at the D0 detector. Namely, we require that one of the tagging jets must have $p_\perp > 50$ GeV, while the other must have $p_\perp > 20$ GeV. The rapidity boost $\bar{y}$ is integrated over, subject to the constraint $|y_1|_{max} = |y_2|_{max} = 3.2$. The rapidity interval is integrated in unit bins centered around the variable y of the plot. Finally, to compare with our previous analysis, we also show in the dashed curves the moments calculated using the kinematic rapidity.

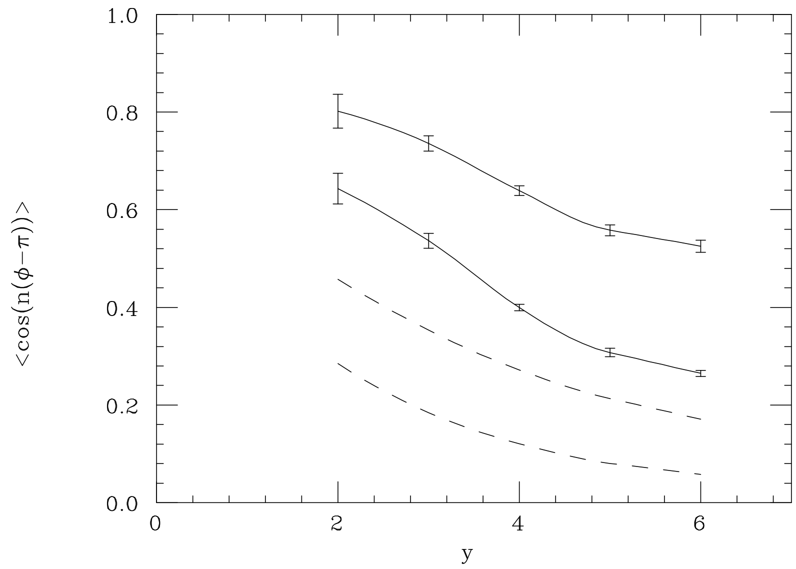

Figure 1: The moments of the azimuthal angle distribution for $n = 1$ and 2, computed with the BFKL resummation using the effective rapidity $\hat{y}$ (solid) and using the kinematic rapidity y (dashed). The error bars are the estimated statistical error from the monte carlo integration.

As expected, the naive BFKL analysis (dashed) tends to overestimate the decorrelation in azimuthal angle. The first two moments are typically two to three times smaller than those calculated using $\hat{y}$ in the BFKL solution (solid). However, there is still a substantial decorrelation exhibited in the solid curves which should be experimentally measurable. For small rapidities one would expect these results to be invalidated by nonleading effects, but for larger rapidities (optimistically, perhaps $y \gtrsim 4$) the minijet effects should begin to dominate. This is a particularly nice process for probing the BFKL structure, from both an experimental and a theoretical point of view. Experimentally, the ϕ measurements are much less affected by detector resolution than the $p_\perp$ measurements [14]. Theoretically, the azimuthal angle distribution is less sensitive to the factorization/renormalization scale used. Thus, a measurement of the azimuthal angle decorrelation should be an excellent probe for the validity range of the BFKL dynamics.

References

[1] S.D. Ellis, Z. Kunszt and D.E. Soper, Phys. Rev. D **40**, 2188 (1989); Phys. Rev. Lett. **64**, 2121 (1990);
F. Aversa, M. Greco, P. Chiappetta and J.Ph. Guillet, Phys. Rev. Lett. **65**, 401 (1990); Z. Phys. C **49**, 459 (1991).

[2] S.D. Ellis, Z. Kunszt and D.E. Soper, Phys. Rev. Lett. **69**, 1496 (1992).

[3] W.T. Giele, E.W.N. Glover, and D.A. Kosower, FERMILAB-Pub-94/070-T (1994).

[4] F. Abe et al., CDF Collab., Phys. Rev. Lett. **68**, 1104 (1992);
F. Abe et al., CDF Collab., Phys. Rev. Lett. **69**, 2896 (1992).

[5] F. Abe et al., CDF Collab., FERMILAB-Conf-93/201-E (1993).

[6] L.N. Lipatov, Yad. Fiz. **23**, 642 (1976) [Sov. J. Nucl. Phys. **23**, 338 (1976)];
E.A. Kuraev, L.N. Lipatov and V.S. Fadin, Zh. Eksp. Teor. Fiz. **71**, 840 (1976) [Sov. Phys. JETP **44**, 443 (1976)]; **72**, 377 (1977) [**45**, 199 (1977)];
Ya.Ya. Balitsky and L.N. Lipatov, Yad. Fiz. **28** 1597 (1978) [Sov. J. Nucl. Phys. **28**, 822 (1978)].

[7] A.H. Mueller and H. Navelet, Nucl. Phys. **B282**, 727 (1987).

[8] V. Del Duca and C.R. Schmidt, Phys. Rev. D **49**, 4510 (1994).

[9] V. Del Duca and C.R. Schmidt, DESY 94-114, SCIPP 94/17, hep-ph 9407359.

[10] W.J. Stirling, DTP/94/04 (1994), hep-ph 9401266.

[11] B.L. Combridge and C.J. Maxwell, Nucl. Phys. **B239**, 429 (1984).

[12] T. Gottschalk and D. Sivers, Phys. Rev. D **21**, 102 (1980);
Z. Kunszt and E. Pietarinen, Nucl. Phys. **B164**, 45 (1980);
F.A. Berends et al., Phys. Lett. **103B**, 102 (1981).

[13] J. Botts et al., MSU-HEP-93/24 (1993).

[14] D0 Collaboration, private communication.